

New light on mitochondrial calcium

Paolo Pinton^a, Marisa Brini^b, Carlo Bastianutto^a, Richard A. Tuft^c, Tullio Pozzan^a and Rosario Rizzuto^{a,*}

^a *Department of Biomedical Sciences, CNR Center for the Study of Biomembranes, University of Padova, Via Colombo 3, 35121 Padova, Italy*

^b *Department of Biochemistry, CNR Center for the Study of Biomembranes, University of Padova, Via Colombo 3, 35121 Padova, Italy*

^c *Biomedical Imaging Group, University of Massachusetts Medical Center, 373 Plantation Street, Worcester, MA 01605, USA*

Received 12 June 1998

Abstract. The possibility of specifically addressing recombinant probes to mitochondria is a novel, powerful way to study these organelles within living cells. We first showed that the Ca^{2+} -sensitive photoprotein aequorin, modified by the addition of a mitochondrial targeting sequence, allows to monitor specifically the Ca^{2+} concentration in the mitochondrial matrix ($[\text{Ca}^{2+}]_m$) of living cells. With this tool, we could show that, upon physiological stimulation, mitochondria undergo a major rise in $[\text{Ca}^{2+}]_m$, well in the range of the Ca^{2+} sensitivity of the matrix dehydrogenases, in a wide variety of cell types, ranging from non excitable, e.g., HeLa and CHO, and excitable, e.g., cell lines to primary cultures of various embryological origin, such as myocytes and neurons. This phenomenon, while providing an obvious mechanism for tuning mitochondrial activity to cell needs, appeared at first in striking contrast with the low affinity of mitochondrial Ca^{2+} uptake mechanisms. Based on indirect evidence, we proposed that the mitochondria might be close to the source of the Ca^{2+} signal and thus exposed to microdomains of high $[\text{Ca}^{2+}]$, hence allowing the rapid accumulation of Ca^{2+} into the organelle. In order to verify this intriguing possibility, we followed two approaches. In the first, we constructed a novel aequorin chimera, targeted to the mitochondrial intermembrane space (MIMS), i.e., the region sensed by the low-affinity Ca^{2+} uptake systems of the inner mitochondrial membrane. With this probe, we observed that, upon agonist stimulation, a portion of the MIMS is exposed to saturating Ca^{2+} concentrations, thus confirming the occurrence of microdomains of high $[\text{Ca}^{2+}]$ next to mitochondria. In the second approach, we directly investigated the spatial relationship of the mitochondria and the ER, the source of agonist-releasable Ca^{2+} in non-excitabile cells. For this purpose, we constructed GFP-based probes of organelle structure; namely, by targeting to these organelles GFP mutants with different spectral properties, we could label them simultaneously in living cells. By using an imaging system endowed with high speed and sensitivity, which allows to obtain high-resolution 3D images, we could demonstrate that close contacts (<80 nm) occur *in vivo* between mitochondria and the ER.

1. Introduction

The possibility of directly monitoring mitochondrial Ca^{2+} concentration in living cells has recently led to a re-evaluation of their role in intracellular Ca^{2+} handling. Using mitochondrially-targeted aequorin, we showed that, upon physiological stimulation with InsP_3 -generating agonists, mitochondria undergo a major rise in the matrix Ca^{2+} concentration ($[\text{Ca}^{2+}]_m$), well in the range of the Ca^{2+} -sensitivity of the matrix dehydrogenases [27–29]. The following work by us and other groups confirmed and extended this unexpected result. In elegant experiments using rhod-2, Hajnoczky et al. showed that, in hepatocytes, the agonist-dependent oscillations of cytosolic Ca^{2+} concentration ($[\text{Ca}^{2+}]_c$), by inducing parallel increases

*Correspondence should be addressed to: Dr Rosario Rizzuto, Department of Biomedical Sciences, University of Padova, Via Colombo 3, 35121 Padova, Italy. Tel.: + 39 049 8276065; Fax: + 39 049 8276049; E-mail: rizzuto@civ.bio.unipd.it.

of $[Ca^{2+}]_m$, control the activity of the Ca^{2+} -dependent dehydrogenases of the matrix, and hence mitochondrial ATP production [14]. This process, besides a direct role in the control of organelle function, appears to play a role in the modulation of the cytosolic signal. Indeed, Jouaville and co-workers showed that the pattern of InsP₃-dependent Ca^{2+} waves of *Xenopus laevis* oocytes is modulated by Ca^{2+} uptake by energized mitochondria [17], and several groups demonstrated the role of mitochondria in buffering cytosolic $[Ca^{2+}]$ changes in neurons [4,20,37,38], adrenal chromaffin [15] and smooth muscle cells [12].

How can the rapid accumulation of Ca^{2+} by mitochondria occur, given the low affinity of their transport mechanisms? Indeed, while the electrochemical potential across the cation-impermeant inner mitochondrial membrane provides a strong driving force for Ca^{2+} accumulation, the ruthenium red-sensitive electrogenic Ca^{2+} uniporter under physiological conditions has markedly low affinity ($K_m \sim 5\text{--}10 \mu\text{M}$) (for a review, see [5,13,26]). At first, based on indirect evidence, we suggested that the mitochondria responded to microdomains of high $[Ca^{2+}]$ generated in their proximity by the opening of the InsP₃-gated channels [28], we then investigated directly this possibility using two different approaches.

We searched for direct evidence for the occurrence of $[Ca^{2+}]$ hotspots on the mitochondrial surface, with aequorin chimera, specifically targeted to the mitochondrial intermembrane space. Then, we aimed at obtaining high resolution images of mitochondria, and of their contacts with the endoplasmic reticulum (ER) in living cells using the targeted chimeras of green fluorescent protein (GFP) and a high-speed imaging system.

2. Results

2.1. Measurement of $[Ca^{2+}]$ mitochondrial in different cell types

The first goal of the present investigation was to analyse the features of the $[Ca^{2+}]$ variations in the mitochondria of different cellular types, using the mitochondrial matrix-addressed aequorin (mtAEQ).

Figure 1 shows the variations of the $[Ca^{2+}]$ of the matrix ($[Ca^{2+}]_m$) induced by different agonists in a variety of cellular types. Reconstitution of aequorin was carried out by incubating transiently transfected cells with coelenterazine [29,30]. The coverslips with the cells were then transferred to the luminometer chamber, and recording was started. At the end of the experiment, the luminescence data were converted into $[Ca^{2+}]$ values using an algorithm based on the Ca^{2+} -response curve of the photoprotein at physiological conditions of pH, $[Mg^{2+}]$, temperature and ionic strength [1]. Panel A refers to data obtained in HeLa cells, and shows that, upon stimulation with an InsP₃-generating agonist, mitochondria undergo a much higher $[Ca^{2+}]$ change than the bulk cytosol. The $[Ca^{2+}]_m$ reaches a maximum value of approximately $10 \mu\text{M}$, then to rapidly return to values close to basal.

The other traces of the figure show that this behaviour is the typical mitochondrial response to an increase in the $[Ca^{2+}]_c$. Indeed, this behaviour is common not only to other cell lines of different embryological origin (cell line 143B originated from human osteosarcoma and the epithelial lines CHO, derived from hamster ovary and the COS derived from monkey kidney) in which the Ca^{2+} release induced by InsP₃ is the main component of the Ca^{2+} signal, but also in the neurons, in which the $[Ca^{2+}]_c$ variations depend on the opening of the plasma membrane channels (such as glutamate-sensitive channels stimulated in the experiment of Fig. 1E). Large increase in $[Ca^{2+}]_m$ is observed also in primary cultures of skeletal muscle myotubes [2] in which Ca^{2+} is released from the sarcoplasmic reticulum via the ryanodine receptor (RyR).

The only exception we found is in the endothelial cell line ECV30 (derived from human umbilical vein). In this case in fact the response in terms of $[Ca^{2+}]_m$ is slower and much smaller than in the

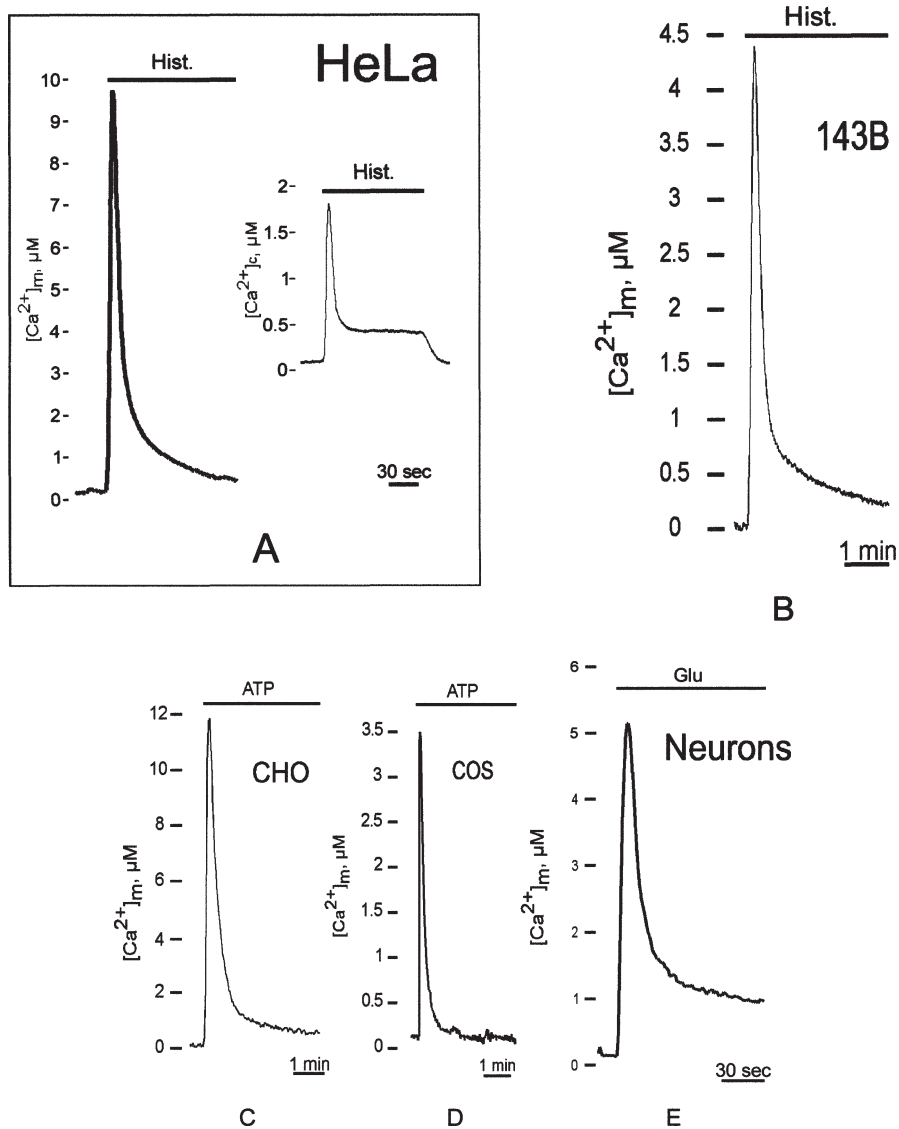


Fig. 1. Effect of agonist stimulation on $[Ca^{2+}]_m$ in various cell type of different embryological origin. After reconstitution of the photoprotein, the coverslips with the cells were transferred to the thermostatted ($37^\circ C$) chamber of the luminometer and perfused with modified Krebs–Ringer buffer, KRB (125 mM NaCl, 5 mM KCl, 1 mM Na_3PO_4 , 1 mM $MgSO_4$, 5.5 mM glucose, 20 mM HEPES, pH 7.4, $37^\circ C$). Where indicated, the cells were treated with 100 μM histamine (Hist.), ATP 100 μM (ATP) or glutamate 200 μM (Glu), added to KRB. In this, and in the following aequorin experiments, the traces are representative of at least five experiments, which gave similar results. Reconstitution of the photoprotein, collection and calibration of the luminescence signal, as well as all other experimental conditions, are described in the Experimental procedures section.

previous measurements; hence in this cellular model the mitochondrial response is similar to the cytosolic one [21].

A direct demonstration that the responses observed with the mtAEQ in Fig. 1 are indeed due to $[Ca^{2+}]$ increasing in the mitochondrial matrix is given by the experiment shown in Fig. 2(a), in which the sensitivity to the mitochondrial uncoupler carbonylcyanide *p*-(trifluoromethoxy) phenylhydrazone (FCCP) of

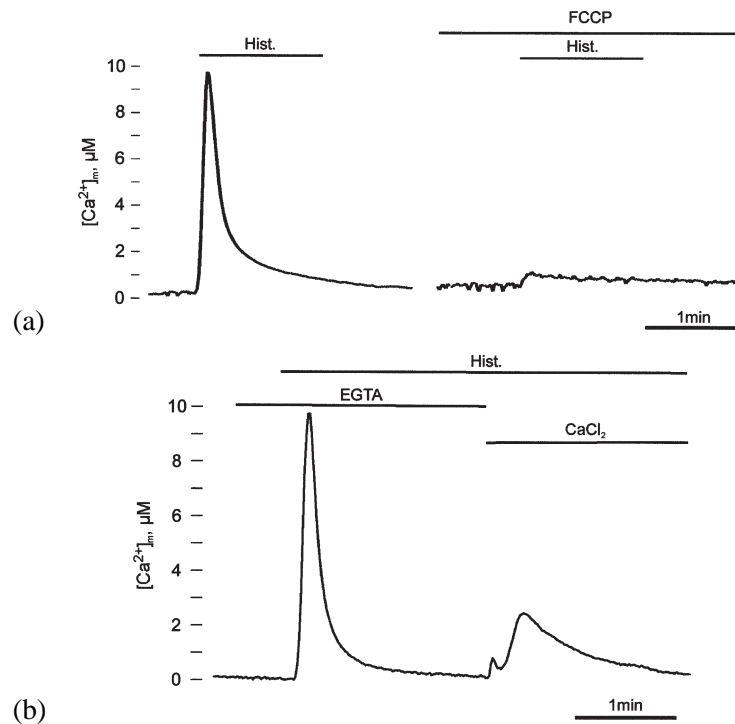


Fig. 2. (a) The effect of the FCCP on the agonist-dependent $[Ca^{2+}]_m$ increases. All conditions as in Fig. 1. Where indicated, the cells were treated with 5 μM carbonylcyanide *p*-(trifluoromethoxy) phenylhydrazone (FCCP) and/or 100 μM histamine (Hist.), added to KRB. (b) The effect of release of Ca^{2+} from the intracellular stores and Ca^{2+} influx on $[Ca^{2+}]_m$. All conditions as in Fig. 1. Where indicated (EGTA), the cells were washed with EGTA 100 μM and then treated with 100 μM histamine (Hist.) added to KRB/EGTA. The medium was then switched with KRB (with 1 mM $CaCl_2$) and, where indicated (Hist.), the cells were challenged with 100 μM histamine (added to KRB).

the $[Ca^{2+}]_m$ has been evaluated. FCCP indeed causes a small decrease in the resting levels of $[Ca^{2+}]_m$, and then almost abolishes the histamine-dependent peak.

In intact cells the high rate of Ca^{2+} mitochondrial uptake after stimulation with agonists coupled to $InsP_3$ generation (or in permeabilized cells, directly stimulated with $InsP_3$), was completely unexpected, given the low affinity of the mitochondrial uniporter. Our explanation for this finding was that the efficiency of mitochondrial Ca^{2+} accumulation could depend on the generation of domains of high $[Ca^{2+}]$ close to the source of the Ca^{2+} rise, which could be sensed by neighbouring mitochondria. To find support for this hypothesis, we evaluated in HeLa cells the relative efficiency of the two pathways for Ca^{2+} increase in the cytosol (Ca^{2+} release from intracellular stores and Ca^{2+} influx from the extracellular medium). In these experiments, the cells were first stimulated with histamine in a medium without $[Ca^{2+}]$ (with EGTA 100 μM), under those conditions the increase of the $[Ca^{2+}]_m$ will be due only to the release of Ca^{2+} from the intracellular stores. The following readdition of Ca^{2+} to the extracellular medium causes a second $[Ca^{2+}]_m$ rise due to the influx through the plasma membrane channels. Exploiting the possibility of observing separately the two mechanisms through which the agonists induce variations in the $[Ca^{2+}]_c$, allows to evaluate the contribution of each mechanism the increase of the $[Ca^{2+}]_m$. As apparent from Fig. 2(b), the release of the Ca^{2+} from the intracellular stores causes a much larger and faster increase on $[Ca^{2+}]_m$ than the influx through the plasma membrane channels. The larger effect on mitochondria of Ca^{2+} released from the ER suggests that a close proximity between these two

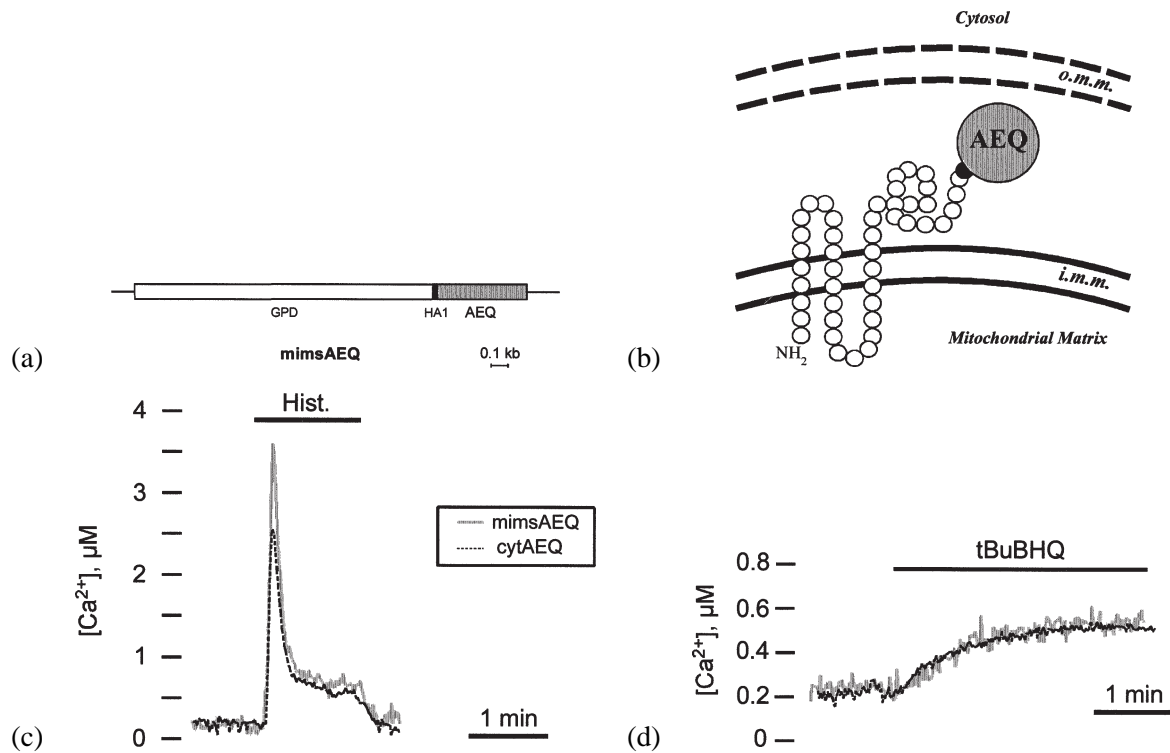


Fig. 3. The aequorin chimera targeted to the mitochondrial intermembrane space (mimsAEQ). (a) Schematic map of the mimsAEQ cDNA. Coding and non-coding regions are represented as boxes and lines, respectively. In the coding region, the portions encoding glycerol-phosphate dehydrogenase (GPD), the HA1 epitope (HA1) and aequorin (AEQ) are white, black and gray respectively. (b) Putative subcellular distribution of the mimsAEQ chimera. Based on the topology of GPD [22], the aequorin moiety is expected to be exposed in the mitochondrial intermembrane space, i.e., between the ion-permeable outer membrane (o.m.m.) and the ion-impermeable inner membrane (i.m.m.). (c) The effect of histamine on the $[Ca^{2+}]_c$ and mitochondrial intermembrane space ($[Ca^{2+}]_{mims}$). The traces show the monitoring of the $[Ca^{2+}]$ of the two compartments in parallel batches of HeLa cells, transiently transfected with the appropriate aequorin chimera (cytAEQ or mimsAEQ). All conditions as in Fig. 1. Where indicated, the cells were treated with 100 μ M histamine (Hist.), added to KRB. (d) The effect of inhibition of the sarco-endoplasmic Ca^{2+} -ATPase (SERCA) on $[Ca^{2+}]_c$ and $[Ca^{2+}]_{mims}$. All conditions as in Fig. 1. Where indicated, the cells were challenged with 10 μ M 2,5-di(tert-butyl)-1,4-benzohydroquinone (tBuBHQ), an inhibitor of the SERCAs [19].

organelles could play a key role in the control of mitochondrial Ca^{2+} homeostasis, and thus organelle function.

2.2. Construction of an aequorin chimera targeted to the intermembrane space of mitochondria (MIMS)

In order to obtain direct experimental evidence in support of this hypothesis, we planned to measure the $[Ca^{2+}]$ in the MIMS, i.e., between the outer mitochondrial membrane, freely permeable to ions and small molecule, and the ion impermeable inner membrane, where the low-affinity mitochondrial Ca^{2+} uniporter is located. For this purpose we constructed a new aequorin chimera, denominated "mitochondrial intermembrane space" (mimsAEQ). To construct this chimera, the cDNA encoding HA1-tagged aequorin was fused in frame with that encoding glycerol phosphate dehydrogenase (GPD) [3], an integral protein of the inner mitochondrial membrane, with a large C-terminal tail (~70% of the molecule)

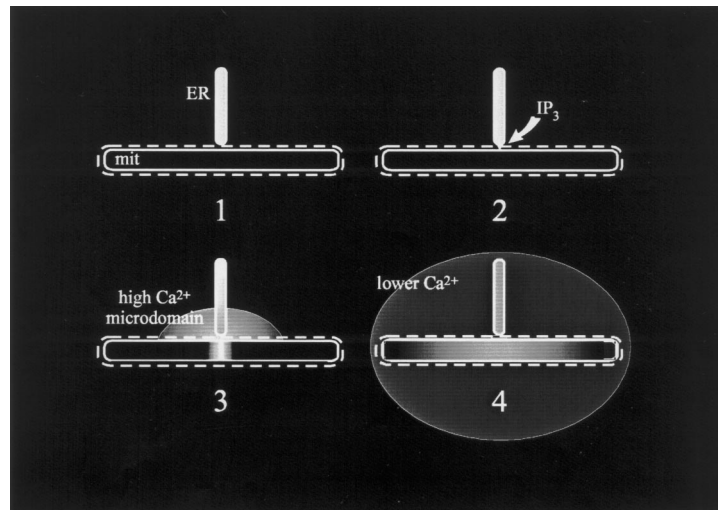


Fig. 4. Schematic model of the role of the tight functional interaction between the ER and the mitochondria in Ca^{2+} signalling. (1) At rest, the ER is endowed with a $[\text{Ca}^{2+}]$ of $\sim 0.5\text{--}1$ mM [16,23–25], whereas the $[\text{Ca}^{2+}]$ of the mitochondrial matrix is similar to that of the bulk cytosol [28,29]. (2) When inositol-1,4,5-trisphosphate (IP_3) is produced following the binding of an agonist to a Gq-coupled receptor, Ca^{2+} is rapidly released from the ER via the InsP_3 receptor, and a microdomain of high $[\text{Ca}^{2+}]$ is generated at the ER/mitochondria contacts. (3) The high local $[\text{Ca}^{2+}]$ allows rapid Ca^{2+} uptake via the low-affinity mitochondrial uniporter, thereby causing a major rise in the $[\text{Ca}^{2+}]$ of the matrix [28,29]. (4) The dissipation of the microdomain at the mouth of the IP_3 -gated channel drastically reduces mitochondrial Ca^{2+} uptake (thereby preventing mitochondrial Ca^{2+} overload) and extends the Ca^{2+} signal to the bulk cytosol, thus activating the Ca^{2+} -sensitive effectors. The early rise in matrix Ca^{2+} , and presumably the diffusion through the mitochondrial network, allows the timely activation of mitochondrial metabolism [14,29,35].

protruding into the intermembrane space [22]. The details of the construction are given in the Experimental procedures section. A schematic map of the final construct is shown in Fig. 3(a), whereas the expected topology is graphically depicted in Fig. 3(b). The encoded polypeptide includes, from the N- to the C-terminus, aa 1–626 of GPD (thus eliminating the EF-type Ca^{2+} -binding site), the HA1 tag and aequorin. The final construct, was transiently expressed in HeLa cells, and evidence for correct localization was sought by immunocytochemistry (not shown).

2.3. The agonist-dependent $[\text{Ca}^{2+}]$ changes of the MIMS are higher than those of the bulk cytosol

The $[\text{Ca}^{2+}]$ in the intermembrane space and for comparison, in the bulk cytosol were then monitored with the appropriate aequorin chimeras. The response to histamine, an agonist coupled to InsP_3 -generation, is shown in Fig. 3(c). In agreement with previous data [1], cytAEQ reveals, upon histamine stimulation of HeLa cells, a transient rise in cytosolic Ca^{2+} concentration ($[\text{Ca}^{2+}]_c$). After the peak ($2.5 \pm 0.3 \mu\text{M}$, $n = 10$), which is mostly contributed by the release of Ca^{2+} from intracellular stores, $[\text{Ca}^{2+}]_c$ declines to a sustained plateau and returns to basal values upon agonist washout. The MIMS shows a comparable behaviour; the peak, however, is significantly higher ($3.5 \pm 0.2 \mu\text{M}$, $n = 10$), and then declines to the same steady-state plateau.

The comparison between the $[\text{Ca}^{2+}]$ variations in the cytosol and MIMS shows since a marked difference only in the first phase, that due to the Ca^{2+} release from the intracellular stores. These data are therefore in accordance with the hypothesis that the opening of the InsP_3 -sensitive channels causes, in the proximity of the mitochondria the generation of cytosolic microdomains, of $[\text{Ca}^{2+}]$ higher than in the

We thus co-expressed mtGFP(Y66H,Y145F) and erGFP(S65T) to obtain 3D images of the mitochondria and the ER *in vivo*, collected serial stacks of images of the two fluorophores and utilized a high-speed (30 ms/image) imaging system based on a low-noise, high-sensitivity back-illuminated cooled CCD camera, which allows a 3D fluorescence image of unprecedented resolution (pixel size ~ 80 nm) to be obtained from computationally deblurred optical sections [33,34]. The result is shown in Fig. 5; the mitochondrial and ER images are represented as pseudocolors (red and green, respectively); the overlaps of the two images (i.e., the 80 nm pixels which include the signal of both fluorophores) are white. Domains of close apposition can be clearly appreciated. The hypothesis that the formation of microdomains with high $[Ca^{2+}]$ sensed by the mitochondria depends on the proximity to ER, is therefore compatible with the image obtained through the analytical system herewith described.

3. Discussion

The study of mitochondrial physiology in intact cells is facing a renewed interest in the last years. Indeed, their capacity to accumulate Ca^{2+} , largely overlooked for some years as a semi-artefactual phenomenon, appears of extreme importance for the control of numerous signalling pathways.

The data obtained have demonstrated that the wide and rapid increase of $[Ca^{2+}]_m$ is the most common response of mitochondria to a cytosolic Ca^{2+} signal. In fact, we have observed a similar behaviour not only in cellular types (such as HeLa, 143B, CHO, COS) in which different agonists act through the production of $InsP_3$ and the consequent release of Ca^{2+} from the ER, but also in primary cultures of neurons, after activation of specific channels of the plasma membrane (such as the glutamate ionotropic receptors). Whatever mechanism is responsible (generation of microdomains with high Ca^{2+} in the proximity of the mitochondria, different affinity *in vivo* of the mitochondrial calcium transport, etc.), this rapid increase, which significantly amplifies the cytosolic response and returns to the basal values more quickly than the cytosol, represents therefore a general phenomenon that, presumably, rapidly tunes mitochondrial metabolism to the increased energetic needs of a stimulated cell.

As to the mechanism allowing the fast mitochondrial response, in HeLa cells the high sensitivity of mitochondria to the release of Ca^{2+} from the ER suggests that, at least in this cell type, close contacts with the ER could be responsible for generating domains of high Ca^{2+} next to mitochondria.

In support of this hypothesis, by using an ultrafast imaging system, which allows a high-resolution solving of the 3D structure of intracellular organelles we have provided a high-resolution view of mitochondria and ER in living cells, each forming an interconnected network, with a restricted number of close contacts (< 80 nm apart). The existence of close appositions between the ER and the mitochondria is consistent with the hypothesis that the efficiency of Ca^{2+} accumulation by the latter organelles *in vivo* depends on their capacity to sense the microdomains of high $[Ca^{2+}]$ generated at the mouth of the $InsP_3$ gated channels, but clearly does not prove it. Direct evidence for the existence of such microdomains on the outer surface of the inner mitochondrial membrane is provided by the functional results obtained with mimsAEQ. This Ca^{2+} probe is strategically located to sense these microdomains and the apparent mean $[Ca^{2+}]$ values monitored with this aequorin have been found to be consistently higher than in the bulk cytosol.

The combination of the morphological and functional data suggests that only a small fraction of the MIMS experiences a higher $[Ca^{2+}]$ upon $InsP_3$ induced Ca^{2+} mobilisation. By calculating how much extra mimsAEQ is consumed compared to cytAEQ during an histamine challenge ($\sim 3-5\%$) one can thus obtain the lower estimate of the surface of mitochondria exposed to high $[Ca^{2+}]$ microdomains. If $[Ca^{2+}]$

in these microdomains was as high as to cause complete discharge of all aequorin in that compartment, the hotspots should correspond to $\sim 3\text{--}5\%$ of the MIMS a value which is in good agreement with the estimate of the apposition sites between mitochondria and ER.

In conclusion, the development of a novel approach to the measurement of mitochondrial Ca^{2+} , in living cells, based on the specific targeting of the Ca^{2+} sensitive photoprotein aequorin, has allowed to obtain new and unexpected information, which brings the mitochondria back to the stage of Ca^{2+} signalling. Indeed the data show not only that, upon cell stimulation, mitochondria undergo changes in matrix $[\text{Ca}^{2+}]$ in the range of the sensitivity of the Ca^{2+} -sensitive dehydrogenases of the Krebs cycle, but also that mitochondrial response depend on local signalling, a major and only partly understood phenomenon in Ca^{2+} -mediated signal transduction.

4. Experimental procedures

4.1. Construction of aequorin and GFP chimeras

mtAEQ [27], cytAEQ [1], mtGFP(Y66H,Y145F) [31,32] and erGFP were already available in the lab. For constructing the mimsAEQ chimera, the ClaI/EcoRI fragment encoding HA1-tagged aequorin [1] was inserted downstream of the internal ClaI site of the glycerolphosphate dehydrogenase (GPD) cDNA. By this means, the two cDNAs were fused in frame, and thus the encoded polypeptide includes aa 1–626 of GPD, the 9 aa HA1 tag and aequorin.

4.2. Cell culture and transfection

HeLa cells were grown in Dulbecco's modified Eagle's medium (DMEM), supplemented with 10% fetal calf serum (FCS) in 75 cm² Falcon flasks. In transient expression experiments, the cells were seeded onto glass coverslips, diameter either 13 mm (for aequorin measurements) or 24 mm (for GFP detection), and allowed to grow to 50% confluence. At this stage, transfection with the appropriate plasmid (4 μg and 8 μg for 13 and 24 mm coverslips, respectively) was carried out as previously described [30]. In the case of mimsAEQ, 0.5 μg of plasmid DNA were employed for the transfection (13 mm coverslip), as we noticed, with high levels of expression, a significant alteration in mitochondrial morphology (rounding up, collapse of the organelle towards the nuclear membrane, etc.). The cells were analyzed for aequorin or GFP expression 36 h after transfection.

4.3. Aequorin measurements

The experiments with the targeted aequorin chimeras were carried out as previously described [29,30]. In brief, 36 h after transfection with the appropriate aequorin expression plasmid, the coverslip with the cell was incubated with 5 μM coelenterazine for 1–2 h in DMEM supplemented with 1% FCS, and then transferred to the perfusion chamber of a purpose-built luminometer [8,30]. The aequorin luminescence signal, collected by a low-noise photomultiplier and stored, via a Thorn-EMI photon counting board, in a 486 IBM-compatible computer, was converted off-line into $[\text{Ca}^{2+}]$ by an algorithm based on the Ca^{2+} affinity of aequorin at physiological conditions of pH, $[\text{Mg}^{2+}]$, ionic strength and temperature [1].

4.4. GFP detection

For the high-resolution 3D images a high speed imaging system was employed, which allows a whole stack of 40 serial images to be collected in <1 s and thus minimizes distortions due to organelle motion, is based on laser illumination and a low-noise frame transfer CCD camera. In double labelling experiments (erGFP(S65T) + mtGFP(Y66H, Y145F)) of Fig. 5, at each z section the sample was alternatively illuminated with UV and blue light and the emitted light filtered by a two-band filter. The two images were then independently collected and separately processed. Thank to a high-speed shutter, also in these experiments the acquisition time of a 40 plane stack was very short (<2 s). The wide-field images were then deblurred using the image restoration software developed by the Biomedical Imaging Group [6].

Acknowledgements

We would like to thank G. Ronconi and M. Santato for technical assistance. This work was supported by grants from “Telethon” (845, 850), from the “Human Frontier Science Program”, from the E.U. “Biomed” program (BMH4CT960181), from the “Armenise Foundation” (Harvard), from the Italian University Ministry, from NATO and from the British Research Council to R.R. and T.P.

References

- [1] M. Brini, R. Marsault, C. Bastianutto, J. Alvarez, T. Pozzan and R. Rizzuto, Transfected aequorin in the measurement of cytosolic Ca^{2+} concentration ($[\text{Ca}^{2+}]_c$): a critical evaluation, *J. Biol. Chem.* **270** (1995), 9896–9903.
- [2] M. Brini, F. De Giorgi, M. Murgia, R. Marsault, M.L. Massimino, M. Cantini, R. Rizzuto and T. Pozzan, Subcellular analysis of Ca^{2+} homeostasis in primary cultures of skeletal myotubes, *Mol. Cell. Biol.* **8** (1997), 129–143.
- [3] L.J. Brown, M.J. MacDonald, D.A. Lehn and S.M. Moran, Sequence of rat mitochondrial glycerol-3-phosphate dehydrogenase cDNA. Evidence for EF-hand calcium-binding domains, *J. Biol. Chem.* **269** (1994), 14 363–14 366.
- [4] S.L. Budd and D.G. Nicholls, A re-evaluation of the role of mitochondria in neuronal Ca^{2+} homeostasis, *J. Neurochem.* **66** (1996), 403–411.
- [5] E. Carafoli, Intracellular calcium homeostasis, *Annu. Rev. Biochem.* **56** (1987), 395–433.
- [6] W.A. Carrington, R.M. Lynch, E.D. Moore, G. Isenberg, K.E. Fogarty and F.S. Fay, Superresolution three-dimensional images of fluorescence in cells with minimal light exposure, *Science* **268** (1995), 1483–1487.
- [7] M. Chalfie, Y. Tu, G. Euskirchen, W.W. Ward and D.C. Prasher, Green fluorescent protein as a marker for gene expression, *Science* **263** (1994), 802–805.
- [8] P.H. Cobbold and J.A.C. Lee, Aequorin measurement of cytoplasmic free calcium, in: *Cellular Calcium. A Practical Approach*, J.G. McCormack and P.H. Cobbold, eds, Oxford University Press, Oxford, UK, 1991, pp. 55–81.
- [9] N.B. Cole, C.L. Smith, N. Sciaky, M. Terasaki, M. Edidin and J. Lippincott-Schwartz, Diffusional mobility of Golgi proteins in membranes of living cells, *Science* **273** (1996), 797–801.
- [10] A.B. Cubitt, R. Heim, S.R. Adams, A.E. Boyd, L.A. Gross and R.Y. Tsien, Understanding, improving and using green fluorescent proteins, *Trends Biochem. Sci.* **20** (1995), 448–455.
- [11] F. De Giorgi, M. Brini, C. Bastianutto, R. Marsault, M. Montero, P. Pizzo, R. Rossi and R. Rizzuto, Targeting aequorin and green fluorescent protein to intracellular organelles, *Gene* **173** (1996), 113–117.
- [12] R.M. Drummond and F.S. Fay, Mitochondria contribute to Ca^{2+} removal in smooth muscle cells, *Pflugers Arch.* **431** (1996), 473–482.
- [13] K.K. Gunter and T.E. Gunter, Transport of calcium by mitochondria, *J. Bioenerg. Biomembr.* **26** (1994), 471–485.
- [14] G. Hajnoczky, L.D. Robb-Gaspers, M.B. Seitz and A.P. Thomas, Decoding of cytosolic calcium oscillations in the mitochondria, *Cell* **82** (1995), 415–424.
- [15] J. Herrington, Y.B. Park, D.F. Babcock and B. Hille, Dominant role of mitochondria in clearance of large Ca^{2+} loads from rat adrenal chromaffin cells, *Neuron* **16** (1996), 219–228.
- [16] A.M. Hofer and I. Schulz, Quantification of intraluminal free [Ca] in the agonist-sensitive internal calcium store using compartmentalized fluorescent indicators: some considerations, *Cell Calcium* **20** (1996), 235–242.

- [17] L.S. Jouaville, F. Ichas, E.L. Holmuhamedov, P. Camacho and J.D. Lechleiter, Synchronization of calcium waves by mitochondrial substrates in *Xenopus laevis* oocytes, *Nature* **377** (1995), 438–441.
- [18] C. Kaether and H.H. Gerdes, Visualization of protein transport along the secretory pathway using green fluorescent protein, *FEBS Lett.* **369** (1995), 267–271.
- [19] G.E.N. Kass, S.K. Duddy, G.A. Moore and S.A. Orrenius, 2,5-di(tert-butyl)-1,4-benzohydroquinone rapidly elevates cytosolic Ca^{2+} concentration by mobilizing the inositol 1,4,5-trisphosphate-sensitive Ca^{2+} pool, *J. Biol. Chem.* **264** (1989), 15 192–15 198.
- [20] L. Kiedrowski and E. Costa, Glutamate-induced destabilization of intracellular calcium concentration homeostasis in cultured cerebellar granule cells: role of mitochondria in calcium buffering, *Mol. Pharmacol.* **47** (1995), 140–147.
- [21] A.M. Lawrie, R. Rizzuto, T. Pozzan and A.W.M. Simpson, A role for calcium influx in the regulation of mitochondrial calcium in endothelial cells, *J. Biol. Chem.* **271** (1996), 10 753–10 759.
- [22] M.J. MacDonald and L.J. Brown, Calcium activation of mitochondrial glycerol phosphate dehydrogenase restudied, *Arch. Biochem. Biophys.* **326** (1996), 79–84.
- [23] A. Miyawaki, J. Llopis, R. Heim, J.M. McCaffery, J.A. Adams, M. Ikura and R.Y. Tsien, Camaleons: fluorescent indicators for Ca^{2+} based on green fluorescent proteins and calmodulin, *Nature* **388** (1997), 882–887.
- [24] M. Montero, M. Brini, R. Marsault, J. Alvarez, R. Sitia, T. Pozzan and R. Rizzuto, Monitoring dynamic changes in free Ca^{2+} concentration in the endoplasmic reticulum of intact cells, *EMBO J.* **14** (1995), 5467–5475.
- [25] M. Montero, M.J. Barrero and J. Alvarez, $[\text{Ca}^{2+}]$ microdomains control agonist-induced Ca^{2+} release in intact HeLa cells, *FASEB J.* (1997) (in press).
- [26] T. Pozzan, R. Rizzuto, P. Volpe and J. Meldolesi, Molecular and cellular physiology of intracellular Ca^{2+} stores, *Physiol. Rev.* **74**(3) (1994), 595–636.
- [27] R. Rizzuto, A.W.M. Simpson, M. Brini and T. Pozzan, Rapid changes of mitochondrial Ca^{2+} revealed by specifically targeted recombinant aequorin, *Nature* **358** (1992), 325–328.
- [28] R. Rizzuto, M. Brini, M. Murgia and T. Pozzan, Microdomains of cytosolic Ca^{2+} concentration sensed by strategically located mitochondria, *Science* **262** (1993), 744–747.
- [29] R. Rizzuto, C. Bastianutto, M. Brini, M. Murgia and T. Pozzan, Mitochondrial Ca^{2+} homeostasis in intact cells, *J. Cell Biol.* **126** (1994), 1183–1194.
- [30] R. Rizzuto, M. Brini, C. Bastianutto, R. Marsault and T. Pozzan, Photoprotein mediated measurement of $[\text{Ca}^{2+}]$ in mitochondria of living cells, *Meth. Enzymol.* **260** (1995), 417–428.
- [31] R. Rizzuto, M. Brini, P. Pizzo, M. Murgia and T. Pozzan, Chimeric green fluorescent protein: a new tool for visualizing subcellular organelles in living cells, *Curr. Biol.* **5** (1995), 635–642.
- [32] R. Rizzuto, M. Brini, F. De Giorgi, R. Rossi, R. Heim, R.Y. Tsien and T. Pozzan, Double labelling of subcellular structures with organelle-targeted GFP mutants *in vivo*, *Curr. Biol.* **6** (1996), 183–188.
- [33] R. Rizzuto, P. Pinton, W. Carrington, F.S.F. Fay, K.E. Fogarty, L.M. Lifshitz, R.A. Tuft and T. Pozzan, Close contacts with the endoplasmic reticulum as determinants of mitochondrial Ca^{2+} responses, *Science* **280** (1998), 1763–1766.
- [34] R. Rizzuto, W. Carrington and R.A. Tuft, Digital imaging microscopy of living cells, *Trends Cell Biol.* (1998) (in press).
- [35] G.A. Rutter, J.M. Theler, M. Murgia, C.B. Wollheim, T. Pozzan and R. Rizzuto, Stimulated Ca^{2+} influx raises mitochondrial free Ca^{2+} to supramicromolar levels in a pancreatic b-cell line, *J. Biol. Chem.* **268** (1993), 22 385–22 390.
- [36] K. Subramanian and T. Meyer, Calcium induced restructuring of nuclear envelope and endoplasmic reticulum calcium stores, *Cell* **89** (1997), 963–971.
- [37] J.L. Werth and S.A. Thayer, Mitochondria buffer physiological calcium loads in cultured rat dorsal root ganglion neurons, *J. Neurosci.* **14** (1994), 348–356.
- [38] R.J. White and I.J. Reynolds, Mitochondria and $\text{Na}^+/\text{Ca}^{2+}$ exchange buffer glutamate-induced calcium loads in cultured cortical neurons, *J. Neurosci.* **15** (1995), 1318–1328.